

Vapor Phase Transport Synthesis of Zeolites from Sol-Gel Precursors

Steven G. Thoma, Tina M. Nenoff*

Sandia National Laboratories

Catalysis and Chemical Technologies Dept.

PO Box 5800, MS 0710

Albuquerque, NM 87185-0710

RECEIVED
AUG 17 2000
OSTI

*Author to whom correspondence should be addressed.

tmnenof@sandia.gov

(505) 844-0340

DISCLAIMER

This report was prepared as an account of work sponsored by an agency of the United States Government. Neither the United States Government nor any agency thereof, nor any of their employees, make any warranty, express or implied, or assumes any legal liability or responsibility for the accuracy, completeness, or usefulness of any information, apparatus, product, or process disclosed, or represents that its use would not infringe privately owned rights. Reference herein to any specific commercial product, process, or service by trade name, trademark, manufacturer, or otherwise does not necessarily constitute or imply its endorsement, recommendation, or favoring by the United States Government or any agency thereof. The views and opinions of authors expressed herein do not necessarily state or reflect those of the United States Government or any agency thereof.

DISCLAIMER

Portions of this document may be illegible in electronic image products. Images are produced from the best available original document.

Abstract

A study of zeolite crystallization from sol-gel precursors using the vapor phase transport synthesis method has been performed. Zeolites (ZSM-5, ZSM-48, Zeolite P, and Sodalite) were crystallized by contacting vapor phase organic or organic-water mixtures with dried sodium silicate and dried sodium alumino-silicate gels. For each precursor gel, a ternary phase system of vapor phase organic reactant molecules was explored. The vapor phase reactant mixtures ranged from pure ethylene diamene, triethylamine, or water, to an equimolar mixture of each. In addition, a series of gels with varied physical and chemical properties were crystallized using the same vapor phase solvent mixture for each gel. The precursor gels and the crystalline products were analyzed via Scanning Electron Microscopy, Electron Dispersive Spectroscopy, X-ray mapping, X-ray powder diffraction, nitrogen surface area, Fourier Transform Infrared Spectroscopy, and thermal analyses. The product phase and purity as a function of the solvent mixture, precursor gel structure, and precursor gel chemistry is discussed.

1. Introduction

Crystallization of zeolites via the introduction of an aqueous-organic vapor mixture with an amorphous, dry gel was presented by Xu, et al., [1] as a means to reduce the consumption of organic materials. This method of synthesis is now generally referred to as vapor phase transport (VPT). The product morphology derived from VPT crystallization of sodium alumino-silicate gels has been found to be a complex function of many factors. These include reaction time and temperature, the relative amounts of sodium, aluminum,

silicon, and quaternary amine in the precursor gel, as well as the type and relative amounts of organic molecules and water in the vapor phase [2-3]. The homogeneity of the precursor gel can also affect product morphology, though the form of the sodium, aluminum, and silicon precursors used to synthesize this gel may not [2].

Although it has been demonstrated that VPT is an alternative means of zeolite synthesis, the underlying mechanism of nucleation and growth is not fully understood. Kim, et al., [2] suggested that water vapor condenses in the precursor gel micropores and establishes a liquid-vapor equilibrium with the organic vapor phases. The pH within the liquid phase is largely a function of the organic molecules used. Silica is dissolved from the walls of the micropores and interacts with the organo-cation, nucleation occurs, and the crystals grow outward toward the surface of the gel. Precursor homogeneity in such a system is very important due to the lack of molecular long-range transport. However, Matsukata, et al., [3] performed VPT crystallizations in systems containing insufficient water to allow condensation under the given reaction conditions, yet zeolite crystallization still occurred. It was concluded that while the role of water is still not fully understood, though its presence greatly enhances the rate of crystallization.

By performing VPT crystallization of differentially aged gels on various substrates Jung, et al., [4] determined that the source for nucleation in VPT crystallization is tetrapropylammonium (TPA) -silica composite structures, which is the same crystallization mechanism that has been proposed for hydrothermal systems [5-11]. This study used only water in the vapor phase, and the organo-cation, TPA, was included in the precursor gel during synthesis. Also, their precursor gels had a substantially higher water content than the precursor gels used elsewhere [2-3].

Other studies involving the crystallization of zeolites from dried alumino-silicate gels [12] and dried boro-silicate gels [13] containing quaternary amines and using only water in the vapor phase showed that phase selection and crystallization rate was strongly influenced by silicon/metal and quaternary amine/silicon ratios. In addition, ZnAPO-34 was crystallized using triethylene from both dried gels via VPT and via hydrothermal synthesis. It was found that in the VPT system, the triethylene/water ratio had no effect on the product morphology and that substituting ethanol for water during either the gel synthesis or in the vapor phase solvent mixture yielded only amorphous products. [14]

In this study, we examine the role of inorganic gel chemistry, inorganic gel structure, and organo-cations in VPT synthesis of zeolites using a sodium silicate system and a sodium alumino-silicate system. Zeolites were crystallized using a vapor phase that ranged from an equimolar mixture of ethylene diamene (En), triethylamine (Et₃N), and water (H₂O), to pure solvent. These organic molecules were chosen because they have been used in previous studies of VPT zeolite crystallization [2,3,14]. In order to ascertain if gel structure influences product morphology during VPT crystallization, precursor gels were prepared both (1) with and without TPA cations, (2) aged and non-aged, (3) dried at both 50 °C and 550 °C. Each of these gels was then subjected to the same VPT crystallization procedure. Precursor gels and products are characterized and the roles of organo-cations, aluminum, water, and the gel structure on VPT crystallization is discussed.

2. Experimental

2.1 Synthesis

Precursor gels were prepared by the addition of sodium nitrate (NaNO_3), aluminum nitrate ($\text{Al}(\text{NO}_3)_3 \cdot 9\text{H}_2\text{O}$), and tetrapropylammonium bromide (TPABr) to a solution of tetraethylorthosilicate (TEOS), ethanol (EtOH), water (H_2O), and hydrochloric acid (HCl). The clear, homogeneous solutions were placed in sealed vials and held at $50\text{ }^\circ\text{C}$ for 48 hours. In each case a clear, rigid gel with no free liquid was obtained. The gel was dried in air at $50\text{ }^\circ\text{C}$ overnight and then ground to a fine powder. The gels are hereafter referred to by their components, such as sodium aluminosilicate with TPA = NaAlSiTPA . The elemental content of these gels is presented as molar ratios in Table 1.

Aged gels were prepared in a similar manner except that prior to drying at $50\text{ }^\circ\text{C}$ they were left at room temperature for 7 days. These gels are hereafter referred to as NaSi-aged, NaSiTPA-aged, NaSiAl-aged, and NaSiAITPA-aged. In addition, a portion of each of the NaSi, NaSiTPA, NaSiAl, and NaSiAITPA gels was calcined at $550\text{ }^\circ\text{C}$ under oxygen using a ramp rate of $3\text{ }^\circ\text{C}/\text{minute}$ and a four hour hold.

For VPT crystallization, a small amount of gel was placed in a raised teflon holder inside a teflon lined steel autoclave. The configuration of the holder was such that only vapor from the solvent mixture would be able to contact the powdered gel. A mixture of ethylenediamine (En), triethylamine (Et_3N), and water was transferred directly to the bottom of the reaction vessel. The total solvent charge ratio was 0.04 moles of solvent to 0.1 gram of dried gel. For the NaSiTPA and NaSiAITPA gels, a total of thirteen different molar ratios of solvent were tested ranging from pure solvent to an equimolar mixture of each (see Figures 1 and 2). The charged autoclaves were placed in a $175\text{ }^\circ\text{C}$ oven for 7 days, after which the recovered product was water and acetone washed, air dried, and re-ground. In addition, each of the NaSi, NaSiTPA, NaSiAl, and NaSiAITPA gels, their $550\text{ }^\circ\text{C}$ calcined

counterparts, and their aged counterparts were similarly treated, but using only one molar ratio of solvents (the 0.2 En : 0.4 Et₃N: 0.2 H₂O point) and left at temperature for 14 days.

2.2 Characterization

Powder X-Ray diffraction (XRD) data were collected on a Siemens D500 diffractometer using Cu-K α radiation. Percent crystallinity was estimated from comparison of the major XRD peak to that of fully crystalline reference samples. Determination of percent crystallinity on six duplicate samples showed that this method had a standard deviation of 5%. Elemental composition was determined via electron dispersive spectroscopy (EDS) using a JEOL T300 scanning electron microscope (SEM) and Iridium (IXRF Systems) software. Elemental distribution was obtained by X-ray mapping, performed using the EDS system. A series of standards with varying silicon to aluminum ratios (Si/Al) were prepared in similar manner as the NaSiAITPA gel and used to quantify the EDS data. A plot of the actual Si/Al versus the EDS measured Si/Al was linear between 1 and 80 where a plateau was reached. The EDS quantitative Si/Al detection limit was therefore taken to be 80. SEM images were recorded using the same system. Thermal analyses were performed using a TA Instruments SDT 2960 simultaneous Thermo Gravimetric Analyzer – Differential Thermal Analyzer (TGA-DTA). Methods for assessment of weight percent residual solvents and dehydroxylation from TGA-DTA data are reported elsewhere [15]. Surface areas were determined using a Quantachrome Autosorb with nitrogen as the adsorbant. Samples were outgassed under vacuum at 120 °C. Qualitative determination of microporosity was made via inspection of isotherms over the relative pressure range of 10⁻⁵ to 10⁻², and quantitative evaluation made using Deboer analysis of t-plots. Pore size distributions (PSD) and total

pore volumes were calculated from the adsorption branch of the isotherm using the BJH (Barett-Joyner-Halenda) model. Fourier Transform – Infrared (FTIR) spectroscopy was performed using a Perkin-Elmer Spectrum GX FTIR.

3. Results

3.1 Precursor Gel

Physical properties of the precursor gels are given in Table 2. All of the 50 °C dried gels that did not contain TPA displayed microporosity, however only one of the gels that contained TPA was microporous. It is possible that all of the 50 °C dried gels were microporous, but not recorded as such because the microporous regions were blocked by occluded TPA molecules. Evidence that TPA resides in the gel pores comes from the observed increase in surface area and pore volume after calcining the TPA-containing samples. Following calcination at 550 °C the NaSiTPA, NaSi, NaSiAlTPA, and NaSiAl gels had very similar surface areas and PSDs, suggesting that the TPA did not affect the gels' structural evolution during thermal densification. Aging the samples prior to drying allows further condensation reactions to take place, possibly densifying and strengthening the gel structure. Note, that following calcination at 550 °C the aged TPA-free gels retained more surface area as a result of aging than those with TPA. The presence or absence of aluminum did not have a noticeable effect on gel surface area or PSD. Figure 1 gives the PSDs of the 50°C dried NaSiTPA and NaSiAlTPA samples. These PSDs, with a modal pore diameter of about 25 Å, are typical of most of the non-microporous samples presented in Table 1. Exceptions are the 550°C calcined NaSi and NaSiTPA gels, with modal pore diameters of about 15 Å. The PSDs for these two samples were similar to the other non-

microporous gels, but shifted toward smaller diameters. The seven gels that contain micropores had modal pore diameters of 7 Å or less with no pores larger than 10 Å.

Thermal analyses data are presented in Table 2 as percent weight loss due to free solvent and due to dehydroxylation. Dehydroxylation in silica gels is a readily reversible process [15] and so these values represent a qualitative evaluation of the relative hydroxyl content of the gels prior to crystallization. The 50 °C dried gels show less variation in these quantities relative to their 550 °C dried counterparts.

FTIR analyses show that all of the TPA containing gels have a sharp C-H stretch at $\sim 2985\text{ cm}^{-1}$, while the TPA-free gels have only a weak $\sim 2985\text{ cm}^{-1}$ stretch. The observed C-H stretching band was due primarily to the presence of TPA, and to a lesser extent non-hydrolyzed TEOS ethoxy groups. The 2985 cm^{-1} stretch is larger on the aged, TPA-free gels than on the non-aged, suggesting that the aged samples retain more ethoxy groups than the non-aged samples. Otherwise, all of the 50 °C dried gels have very similar FTIR spectra, including an intense 945 cm^{-1} band attributable to Si-OH and SiO-H stretching. After calcining at 550 °C both the 2985 cm^{-1} C-H and the 945 cm^{-1} bands are lost from all samples. Furthermore, only the the TPA-free gels displayed a considerable reduction of intensity of the broad O-H stretching band centered at 3450 cm^{-1} following 550 °C calcining, indicating a much greater degree of dehydroxylation than the TPA containing gels [15].

X-ray mapping of the precursor gels shows that the silicon, aluminum, sodium and chlorine atoms are evenly distributed in all of the gels. However, sodium and chlorine also occur in small pockets of higher concentration which are randomly distributed throughout the gel. The pockets usually contained high concentrations of both elements, but there were instances of high concentration pockets of chlorine alone. XRD analysis indicated that

calcining the gels at 550 °C caused the crystallization of halite. It is interesting to note that following VPT crystallization, no high concentration pockets of sodium or chlorine were found in the remaining amorphous material, nor was there any halite.

3.2 VPT Crystallization

Figures 1 and 2 are ternary phase diagrams that give the phase and percent crystallinity obtained as a function of the vapor phase solvent mixture. Figure 1 presents results for the NaSiTPA gel and Figure 2 for the NaSiAITPA gel. SEM micrographs of products ZSM-5, ZSM-48, and Sodalite are shown in Figure 3a-3c, respectively. While in these examples it appears that the crystals have grown on the gel surface, there is evidence that the crystals grew from within the gel (see Figures 4a-4c). There is no correlation between gel structural characteristics or vapor phase solvent mixture and apparent crystal growth behavior.

ZSM-5 and ZSM-48 occur in similar solvent mixtures with both gels. However, two phases were obtained in the NaSiTPA system which did not occur in the NaSiAITPA system, SOD (Sodalite) and GIS (Zeolite P). SOD occurs in an area of the phase diagram that produced no crystalline product in the NaSiAITPA system, and has a similar XRD pattern to the high silica Sodalite discussed by Sato, et al., [16;17]. The vapor phase solvent mixture location where Zeolite P occurs in the NaSiTPA system corresponds to a 2% crystalline ZSM-5 sample in the NaSiAITPA system. The phase area where no crystalline product was obtained is similar for both systems, and corresponds to the low/no water solvent mixtures.

Figure 5 gives the Si/Al ratio of the crystalline products obtained in the NaSiAlTPA system versus the vapor phase solvent mixture used. The Si/Al ratio clearly varies with solvent mixture, but the variation does not depend on the presence or absence of any single solvent, though the highest Si/Al ratios were obtained at the highest water contents. In general, for the NaSiAlTPA system, both highest aluminum content and highest percent crystallinity occurred with low/no En, low/no Et₃N, and high water.

An interesting observation in the NaSiTPA system is that as the water content of the VPT solvent mixture is increased there is a corresponding increase in the structural complexity of the crystalline products: amorphous ; Sodalite (6 member ring, 1D channels) ; ZSM-48 (10 member ring 1D channels) ; Zeolite P (8 member ring 2D channel); ZSM-5 (10 member rings, 2D channels), respectively. This trend is mirrored in the NaSiAlTPA system but is less obvious due to the absence of Sodalite and Zeolite P.

The percent crystallinity, product morphology, and product silicon to aluminum ratios for the series of gels VPT crystallized at the 0.2 En : 0.4 Et₃N : 0.4 H₂O point are given in Table 3. It can be seen by a comparison between Tables 2 and 3 that there is little correlation between the gels physical properties (directly measured or inferred) and the crystalline products phase or degree of crystallinity. However, the NaSi gels synthesized with TPA were more crystalline than those synthesized without TPA, whether aged/non-aged or 50/550 °C treated, while the opposite is observed for the NaSiAl gels.

FTIR analysis of the 50 °C NaSiAl-aged post reaction gel (which remained fully amorphous) was performed to assess the state of the adsorbed organocations. The relative intensities and locations of C-H and N-H bending bands as well as the Si-NH₂ stretch suggest that there are other organic molecules present besides En, Et₃N, and TPA. This is

consistent with studies which have shown that these molecules may exist in different bonding environments or partially decompose under the temperatures used here [20-23]. The complete lack of the Si-OH, SiO-H, and O-H stretches suggests that these organic species have adsorbed readily onto surface hydroxyl sites.

FTIR analysis was also performed on the balance of the samples, all of which were a mixture of crystalline and amorphous phases. The mixture of phases obviously complicates spectral interpretation and so this data was used only as a basis of comparison between samples of similar crystalline nature and content. Comparisons were made with regard to the relative amount of hydroxyls versus adsorbed organics by analysis of: C-H bends between 1350 and 1600 cm^{-1} [15,21]; Si-NH₂ stretch at 3300 cm^{-1} [15]; N-H bend at 1720 cm^{-1} [23]; Si-OH and SiO-H stretches at 945 cm^{-1} ; O-H stretch at 3450 cm^{-1} [15]. There was no discernable correlation between organic content and either the degree of crystallinity, the product Al:Si ratio, or to the presence or absence of aluminum.

4. Discussion

4.1 Role of Organocation

Differences in morphology due to the use of different organic structure directing agents in hydrothermal synthesis has been attributed to the relative basicity of the organic molecules used and their effect on the pH of the synthesis solution [2,18,19]. In the vapor phase the relative basicity of organic molecules is a measure of the strength of their interaction with surface acid sites. Both En and Et₃N interact strongly with both types of surface acid sites (M-O-M, and M-OH, M = Al, Si), though Et₃N has been observed to adsorb preferentially on hydroxyl sites [20]. Since the presence of aluminum creates

stronger acid sites, we might expect the NaSiAl gels to have a stronger interaction with the vapor phase organocations than their NaSi counterparts. If crystallization was dependent primarily on the strength and extent of adsorption of organocations from the vapor phase, we would expect that the gels that the least crystalline gels would exhibit the least interaction with the organic molecules. However FTIR analysis of post-reaction gels did not yield any evidence to support this. For example, the 50 °C NaSiAl-aged gel showed very strong inorganic-organic interaction, yet it remained amorphous, while on the 550 °C NaSiAl-aged gel (16% crystallinity) there was no indication of adsorbed organics and very strong hydroxyl peaks. This may suggest that the vapor phase organocations, though required for crystallization in the absence of a structure directing agent included in the gel (i.e. TPA), are not the primary factor controlling crystallization.

It is difficult to separate the role of the pore-bound TPA from that of aluminum from this data set because of conflicting trends in the results presented in Table 3. Specifically, the TPA/aluminum containing gels were generally more crystalline than their pure silica counterparts, while the non-TPA/aluminum containing gels were all less crystalline than their pure silica counterparts. If we accept that the presence of aluminum complicates the structure directing effect of the organocations, then the clearest discussion concerning the role of the TPA should be derived from the all silica system. It can be seen from Figure 1 that the NaSiTPA gel produced crystalline products when the VPT solvent was wholly water. When this experiment was repeated using the NaSi (no TPA) gel only amorphous products were obtained, indicating that TPA acts as a structure directing agent in these gels. Hence, if TPA is acting as a structure directing agent in the NaSiTPA system we should see some marked differences between the 50 °C dried NaSiTPA and NaSi gels, but both samples had

similar yields of ZSM-48. This suggests that the structure-directing role of the pore-bound TPA was superseded by the vapor phase organic molecules.

4.2 Role of Aluminum

It has been found in hydrothermal systems that when aluminum is present structure is directed primarily by the aluminosilicate gel chemistry (i.e. the decreased flexibility of the gel framework) and to a lesser extent by the organocations [7,19], which may lead to both decreased crystallinity and crystallization of products with diminished structural complexity [19]. We did not find any systematic relationship between adsorption of organic molecules from the vapor phase and the presence of aluminum in the gels; therefore it is possible that differences in the results between the NaSiAl and NaSi systems are also due to the aluminosilicate gel chemistry. Contrary to this however is a systematic difference in degree of crystallinity between the TPA and the non-TPA gels of the silicate and aluminosilicate systems. As mentioned previously, the TPA/aluminum containing gels were generally more crystalline than their pure silica counterparts, while the non-TPA/aluminum containing gels were all less crystalline than their pure silica counterparts. This discrepancy suggests that the degree of interaction between the inorganic gel and the TPA was greater in the aluminum containing samples.

It is unclear why all four of the NaSiAl 550 °C calcined gels produced the same phases as the 50 °C NaSiAl-TPA gels. It was anticipated that after the loss of TPA due to calcining that the crystallization behavior of these gels would be more like the 50 °C NaSiAl gel (no TPA). It can be seen from Table 2 that the 50 °C NaSiAl gels had substantially different PSDs than did the other NaSiAl gels, tempting us to attribute the difference in crystallinity to the difference in inorganic gel structure. However, the same trend in PSDs is

present in the NaSi system, yet we did not observe the drastic change in product morphologies. The differences in product morphology in the aluminum containing system are therefore due to the presence of aluminum and perhaps its interaction with the organocations, rather than simply an effect of gel PSD. Whether the aluminum alters the crystallization behavior because of increased gel framework rigidity or because of enhanced interaction with organocations cannot be determined from this data.

4.3 Role of Water

While the organocations adsorb onto surface acid sites, water readily cleaves siloxane (Si-O-Si) bonds, as during gel rehydration [15]. Molecular re-arrangement in the covalently bonded gel network would require a significant amount of siloxane (and/or Si-O-Al) bond cleavage. In essence, bond cleavage creates free surface that requires adsorption of solvent from the vapor phase. The role of water in the VPT solvent mixture is therefore likely two-fold: (1) re-hydration of surface siloxane groups to create hydroxyl groups that can act as adsorption sites for the organocations, and (2) to facilitate bond breakage required for molecular rearrangement. In this situation, the adsorption of organocations onto hydroxyl groups may facilitate cleavage of additional siloxane bonds between neighboring silicon atoms by decreasing the covalency of the remaining Si-O-Si bonds. This is consistent with the observation that higher water content led to higher percent crystallinity and increasingly complex crystalline structures (i.e., more molecular water was needed where the highest amount of molecular re-arrangement occurred).

4.4 Role of Gel Structure

All of the aged, 50 °C dried gels were more crystalline than their non-aged 50 °C counterparts. FTIR indicated an increased presence of non-hydrolyzed ethoxy groups in the

aged samples. The role of these ethoxy groups to diminish crystallinity could be the corresponding decreased number of hydroxyl (adsorption) sites, decreased access to adsorption sites due to steric effects, and/or evolution of ethanol from decomposition of these groups during synthesis. Note that this trend is absent for the gels calcined at 550 °C, after the ethoxy groups have been completely removed.

As noted previously, there was no systematic relationship between the inorganic gel surface area and PSD and their crystallization behavior. Clearly, the inorganic gel chemistry, organic molecules, and water play a more prominent role in directing crystallization.

5. Conclusions

Zeolites were crystallized by transporting organic-water mixtures in the vapor phase to a dried sodium silicate or sodium aluminosilicate gels. A range of solvent mixtures and a range of gel chemistries and structures were used to explore the relationship between precursor gels physical properties, VPT solvent mixture, and the VPT crystallization products. The amount of water in the VPT solvent mixture has the greatest effect on crystallization. Increasing amounts of water tend to yield a more crystalline product as well as a more structurally complex product. The type of organic molecule used, and whether included in the precursor gel or introduced via the VPT solvent mixture, has a lesser effect, though the presence of an organic is necessary for crystallization. The presence of aluminum effects the crystallization process, possibly due to changes in rigidity of the gel framework. There was no evidence that the presence of aluminum in the precursor gel enhanced crystallization via increased interaction with the vapor phase organic molecules. Yet it is possible that the aluminum caused enhanced interaction with the pore bound

organocation. Purely structural factors of the gel, such as surface area and pore size distribution do not effect the crystallization process.

Acknowledgements

This work was supported by the United States Department of Energy under Contract DE-AC04-94AL85000. Sandia is a multi-program laboratory operated by Sandia Corporation, a Lockheed Martin Company, for the United States Department of Energy.

References

- [1] W. Xu, J. Dong, J. Li, J Li, and F. Wu, *J. Chem. Soc., Chem. Commun.*, (1990) 755-756.
- [2] M.H. Kim, H.X Li, and M.E. Davis, *Microporous Materials*, 1(1993) 191-200.
- [3] M. Matsukata, N. Nishiyama, and K. Ueyama, *Microporous Materials*, 7 (1996) 109-117.
- [4] M.K. Jung, M.H. Kim, and S.S. Hong, *Microporous and Mesoporous Materials* 26 (1998) 153-159.
- [5] S.L. Burkett and M.E. Davis, *J. Phys. Chem.*, 98 (1994) 4647-4653.
- [6] S.L. Burkett and M.E. Davis, *Chem. Mater.*, 7 (1995) 920-928.
- [7] S.L. Burkett and M.E. Davis, *Chem. Mater.*, 7 (1995) 1453-1463.
- [8] R. Gougeon, L. Delmotte, D. Le Nouen, and Z. Gabelica, *Microporous and Mesoporous Materials* 26 (1998) 143-151.
- [9] P.P.E.A. de Moor, T.P.M. Beelen, R.A. van Santen, K. Tsuji, and M.E. Davis, *Chem. Mater.*, 11 (1999) 36-43.
- [10] T. Nakazawa, M. Sadakata, and T. Okubo, *Microporous and Mesoporous Materials*, 21 (1998) 325-332.
- [11] C.E.A. Kirschhock, R. Ravishankar, F. Verspeurt, P.J. Grobet, P.A. Jacobs, and J.A. Martens, *J. Phys. Chem. B*, 103 (1999) 4965-4971.

- [12] P.R.H.P. Rao, K. Ueyama, and M. Matsukata, *Applied Catalysis A: General* 166 (1998) 97-103.
- [13] R. Bandyopadhyay, Y. Kubota, N. Sugimoto, Y. Fukushima, and Y. Sugi, *Microporous and Mesoporous Materials*, 32 (1999) 81-91.
- [14] L. Zhang and G. R. Gavalas, *Chem. Commun.*, (1999) 97-98.
- [15] C.J. Brinker and G.W. Scherer, *Sol-Gel Science*, Academic Press, Boston, 1990.
- [16] M. Sato, H. Uehara, E. Kojima, and M. Miyake, *Chemistry Letters*, 11 (1995) 1033-1034.
- [17] M. Sato, E. Kojima, H. Uehara, and M. Miyake, *Studies in Surf. Sci. and Catal.*, 105A (1997) 509-516.
- [18] X.W. Guo, G. Li, X.F. Zhang, and X.S. Wang, *Studies in Surface Science and Catalysis*, 112 (1997) 499-508.
- [19] L.D. Rollman, J.L. Schlenker, S.L. Lawton, C.L. Kennedy, G.J. Kennedy, and D.J. Doren, *J. Phys. Chem. B*, 103 (1999), 7175-7183.
- [20] D.W. Jin, K. Onose, H. Furukawa, T. Nitta, and K. Ichimura, *Journal of Chemical Engineering of Japan*, 29 (1996) 139-145.
- [21] K.H. Schnabel, G. Finger, J. Kornatowski, E. Loffler, C. Peuker, and W. Pilz, *Microporous Materials*, 11 (1997) 293-302.
- [22] M.M. Shi, H.Z. Chen, and M. Wang, *J. App. Pol. Sci.*, 64 (1997) 1769-1774.
- [23] B. Sweryda-Frawiec, R.R. Chandler-Henderson, J.L. Coffey, Y.G. Rho, and R.F. pinizzotto, *J. Phys. Chem.*, 100 (1996) 13776-13780.
-

Table 3. Results of gels VPT crystallized at the 0.2 En : 0.4 Et₃N : 0.4 H₂O point

sample	50 °C dried			550 °C calcined		
	phase	% crystalline	Si/Al	phase	% crystalline	Si/Al
NaSiTPA	ZSM-48	85	na	ZSM-48 ZSM-5	1 <1	na
NaSiTPA-aged	ZSM-5	4	na	ZSM-5	5	na
NaSi	ZSM-48	97	na	ZSM-5	96	na
NaSi-aged	ZSM-48	55	na	ZSM-48	100	na
NaSiAITPA	ZSM-5 ZSM-48	51 7	65 77	ZSM-5 ZSM-48	17 <1	73 31
NaSiAITPA-aged	ZSM-5 ZSM-48	40 6	>80 >80	ZSM-5 ZSM-48	86 9	>80 >80
NaSiAl	Zeolite P ZSM-5	6 <1	7 35	ZSM-5 ZSM-48	23 <1	>80 >80
NaSiAl-aged	amorphous	na	na	ZSM-5 ZSM-48	14 2	68 53

Table 2. Physical properties of precursor gels

Gel Sample	50 °C dried					550°C calcined				
	surface area (m ² /g)		pore volume (cc/g)	% weight loss		surface area (m ² /g)		pore volume (cc/g)	% weight loss	
	total	μ-pore		adsorbed/ pore H ₂ O/EtOH	loss of hydroxyls	total	μ-pore		adsorbed/ pore H ₂ O	loss of hydroxyls
NaSiTPA	4	0	9.8e-3	2.7	7.8	4	0	0.5	0.5	20.8
NaSiTPA-aged	15	2	1.6e-2	5.3	9.5	2	0	9.7e-3	3.0	2.4
NaSi	567	240	6.0e-1	8.8	8.1	2	0	1.4e-2	2.4	1.6
NaSi-aged	606	261	7.6e-1	8.4	9.7	45	2	5.3e-2	2.2	1.7
NaSiAITPA	2	0	7.1e-3	4.1	9.4	3	0	1.4e-2	1.4	4.8
NaSiAITPA-aged	<1	0	1.6e-1	4.8	8.9	12	0	2.1e-2	6.5	2.1
NaSiAl	513	217	5.0e-1	4.3	8.1	7	0	2.1e-2	0.5	0.5
NaSiAl-aged	870	380	1.1	3.8	9.8	28	3	5.3e-2	2.3	1.3

Table 1. Molar ratios of precursor gels.

Gel Designation	TEOS	TPABr	NaNO ₃	Al(NO ₃) ₃ ·9H ₂ O	HCl	H ₂ O	EtOH
NaSi	20.7	0	1	0	2.7	164.2	75.8
NaSiTPA	20.7	1	1	0	2.7	164.2	75.8
NaSiAl	20.7	0	1	.01	2.7	164.2	75.8
NaSiAITPA	20.7	1	1	.01	2.7	164.2	75.8

Figure 1.
NaSiTPA system phase and percent crystallinity ternary phase diagram.

Figure 2.
NaSiAITPA system phase and percent crystallinity ternary phase diagram.

Figure 3a.
ZSM-5 growing at gel surface – NaSiAITPA 50 °C dried, crystallized using a solvent ratio of En:Et₃N:H₂O = 0.0:0.5:0.5

Figure 3b.
ZSM-48 growing at gel surface – NaSi-aged 50 °C dried, crystallized using a solvent ratio of En:Et₃N:H₂O = 0.0:0.2:0.4:0.4

Figure 3c.
SOD growing at gel surface – NaSiTPA 50 °C dried, crystallized using a solvent ratio of En:Et₃N:H₂O = 0.33:0.33:0.33

Figure 4a.
ZSM-5 and some ZSM-48 growing beneath gel surface – NaSiAITPA 550 °C calcined, crystallized using a solvent ratio of En:Et₃N:H₂O = 0.2:0.4:0.4

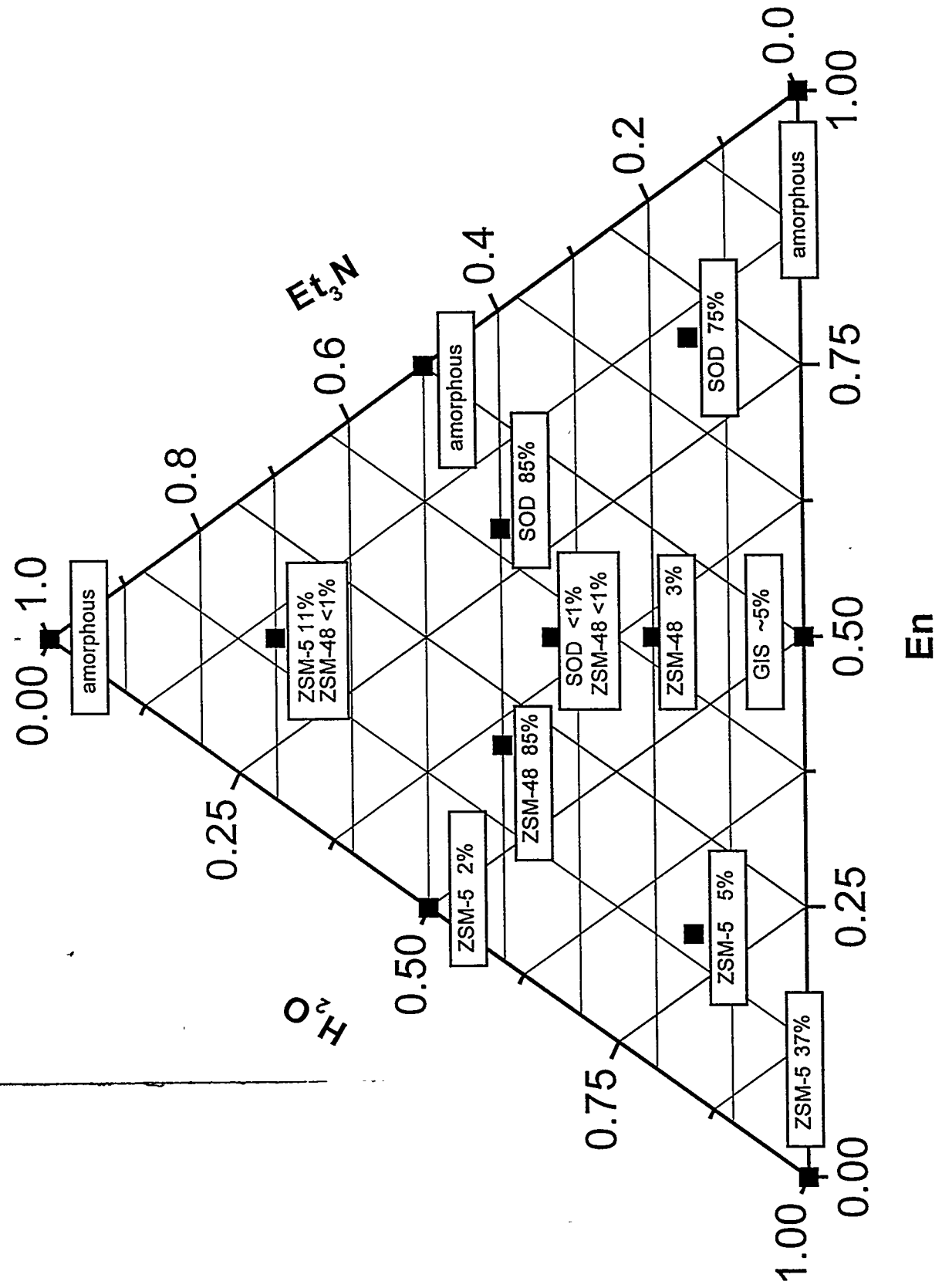
Figure 4b.
ZSM-48 growing beneath gel surface – NaSiTPA 50 °C dried, crystallized using a solvent ratio of En:Et₃N:H₂O = 0.2:0.4:0.4

Figure 4c.
SOD growing beneath gel surface – NaSiTPA 50 °C dried, crystallized using a solvent ratio of En:Et₃N:H₂O = 0.70:0.15:0.15

Figure 5.
NaSiAITPA system phase and Si/Al ratio ternary phase diagram.

Figure 6.
Pore size distribution of 50 °C dried NaSiTPA and NaSiAITPA gels.

Figure 1



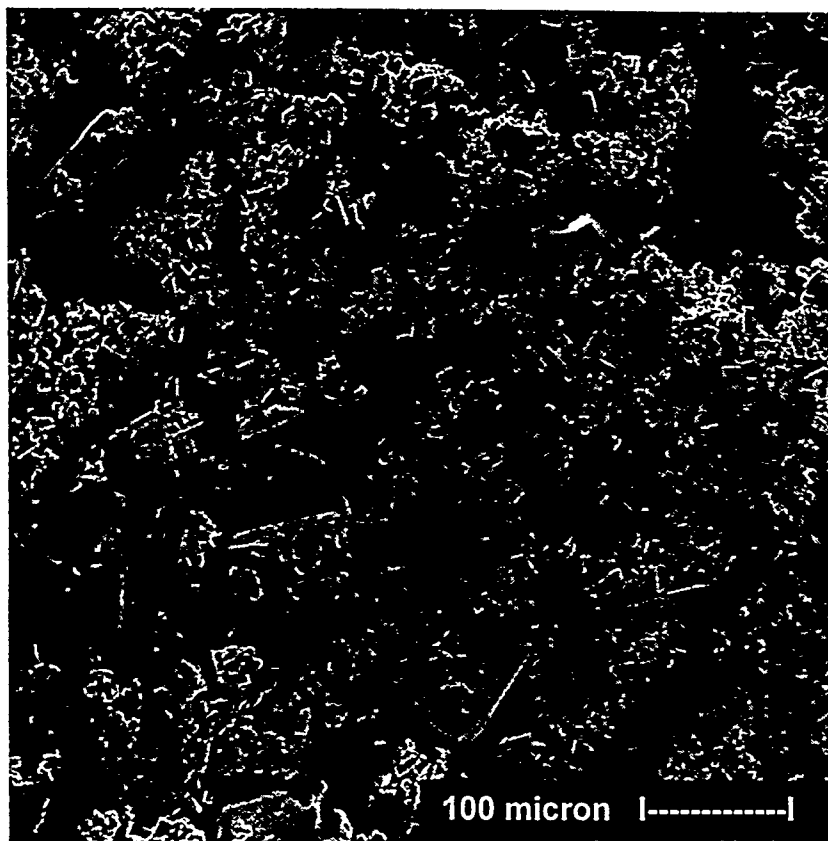


Figure 3a

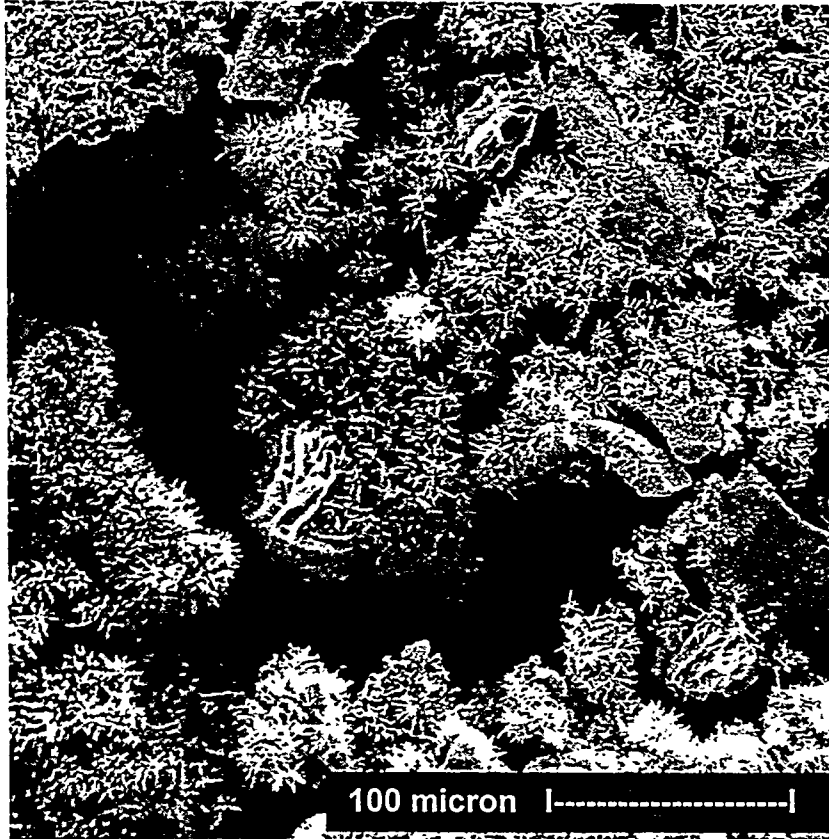


Figure 3b

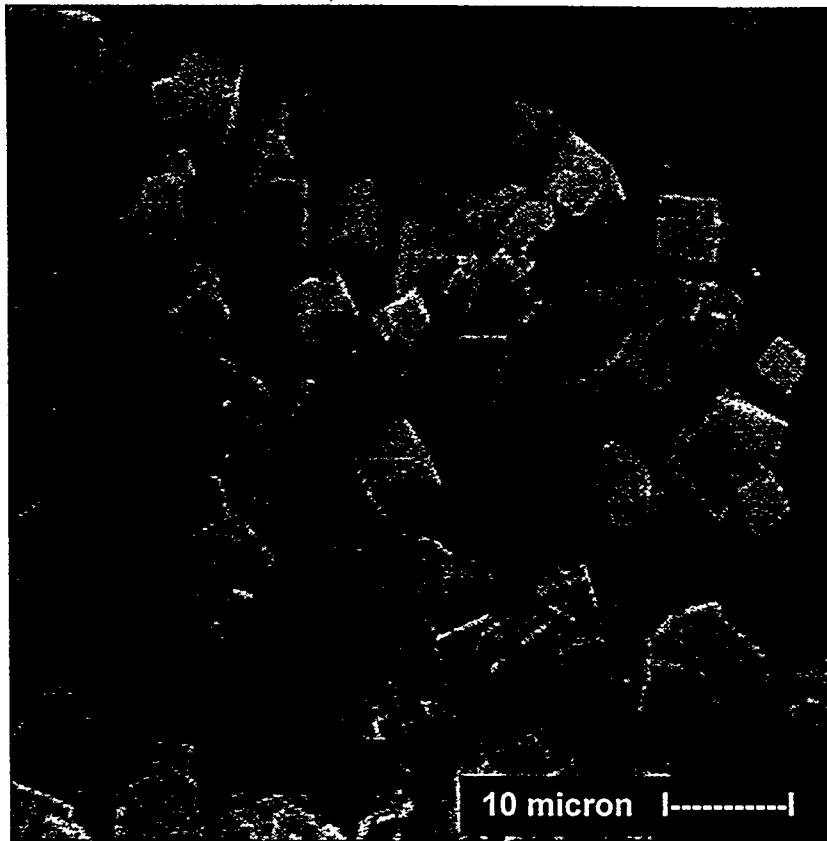


Figure 3c

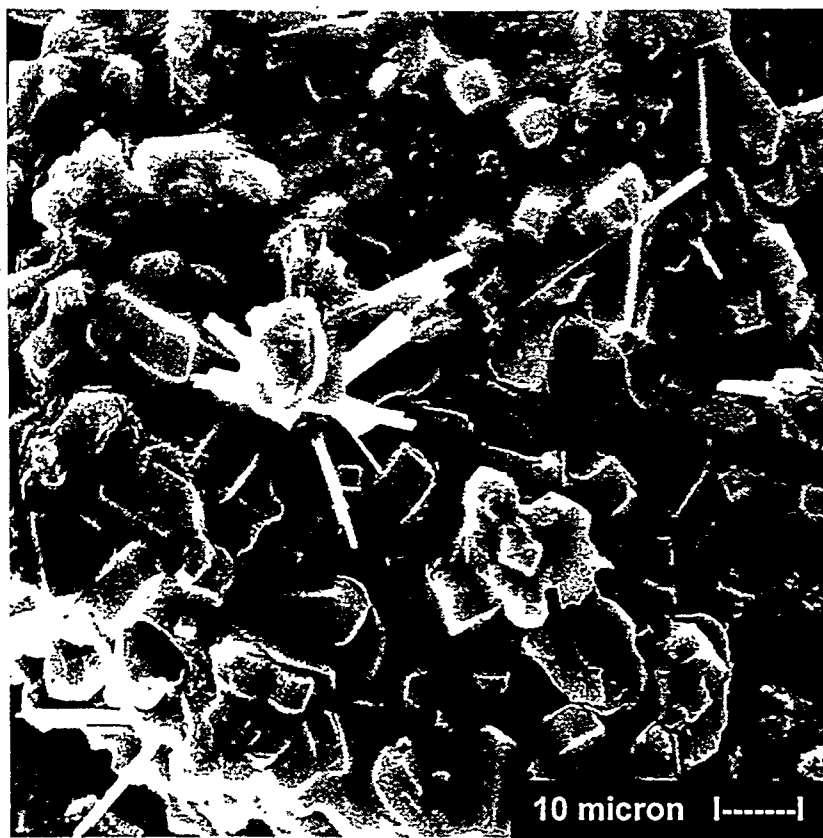


Figure 4a

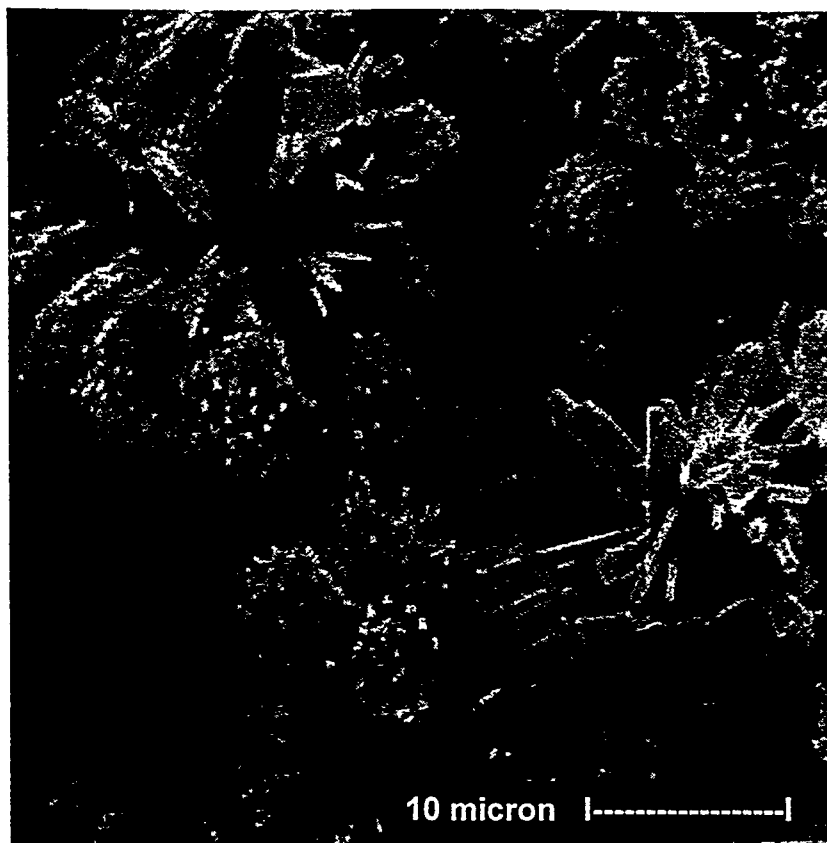


Figure 4b

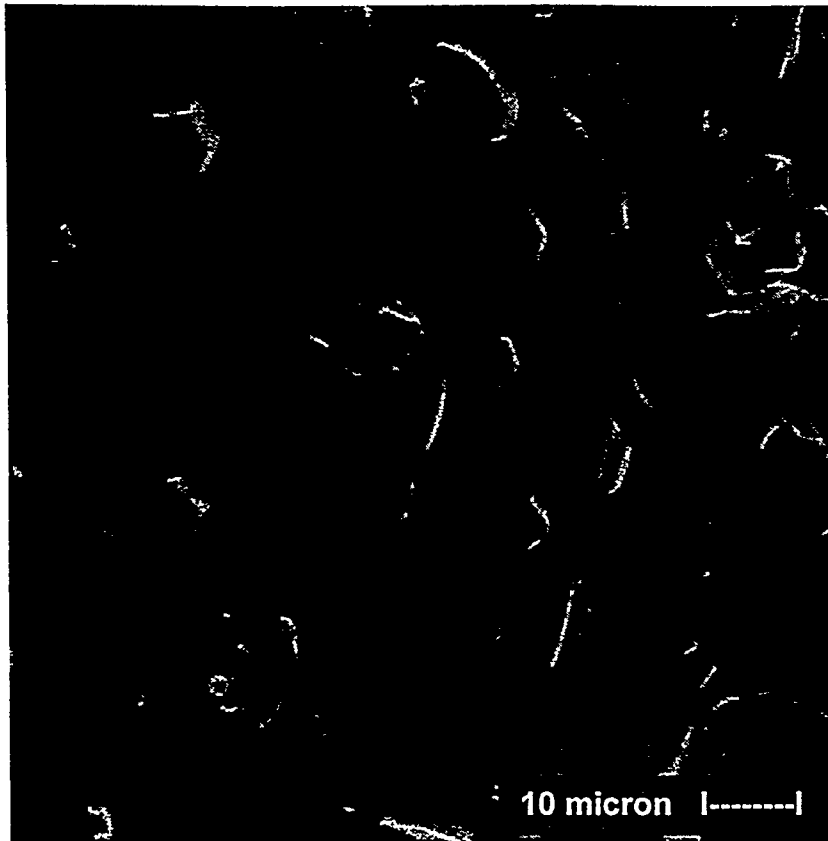
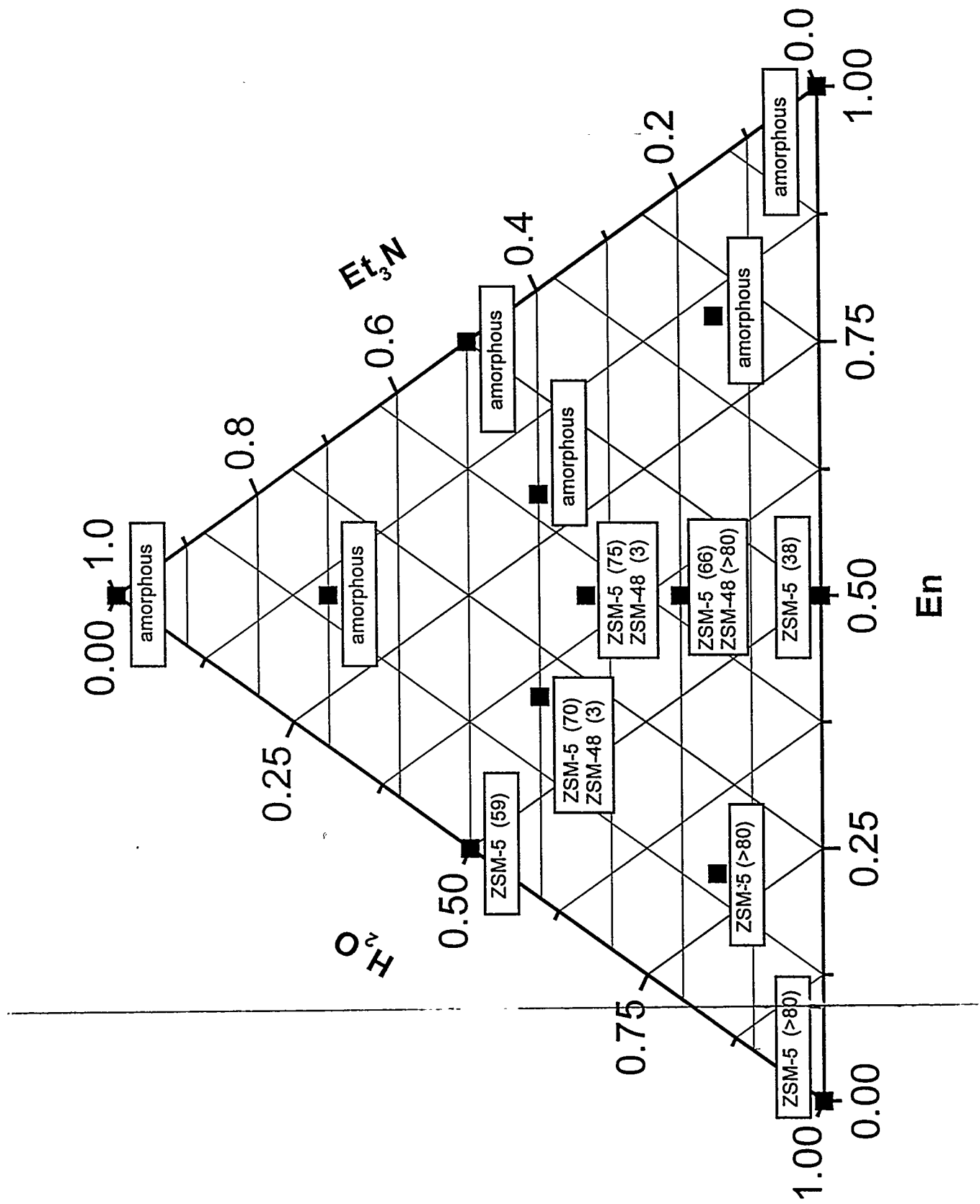


Figure 4c

Figure 5



16.01.6

